

**United States  
Department of  
Agriculture**

**Natural Resources  
Conservation  
Service**

**100 Campus Boulevard  
Suite 200  
Newtown Square, PA 19087-4585**

---

**Subject:** Archaeology -- Geophysical Assistance

**Date:** 16 August 2004

**To:** Margo L. Wallace  
State Conservationist  
USDA-NRCS,  
344 Merrow Road, Suite A  
Tolland, CT 06084-3917

**Purpose:**

A GEM-300 sensor with accessories was transferred from the National Soil Survey Center to the Connecticut Soil Staff. Training on the use and operation of this electromagnetic profiler was provided to the soil staff. In addition, at the request of the Connecticut State Archaeologist and local historians, ground-penetrating radar (GPR) and electromagnetic induction (EMI) surveys were conducted at the Whitfield House (Guilford), Glastonbury Green Cemetery (Glastonbury), Goeffe House (Meriden), and Harriet Beecher Stowe House (Hartford) in an attempt to locate buried cultural features, outbuildings, or unmarked burials.

**Participants:**

Dawn Adiletta, Curator, Harriet Beecher Stowe Center, Hartford, CT  
Reddy Asi, GIS Specialist, Map Collection, Yale University, New Haven, CT  
Nicholas Bellantoni, Connecticut State Archaeologist, Connecticut Archaeology Center, Univ. of Connecticut, Storrs, CT  
Dave Cooke, Archaeologist, FOSA/ABAS, Rocky Hill, CT  
Jim Doolittle, Research Soil Scientist, USDA-NRCS-NSSC, Newtown Square, PA  
Debbie Frigon, Soil Scientist, USDA-NRCS, Tolland, CT  
Fred Gudrian, President, Goeffe House Historical Center, Meriden, CT  
Katherine Kane, Executive Director, Harriet Beecher Stowe Center, Hartford, CT  
Kip Kolesinskas, State Soil Scientist, USDA-NRCS, Tolland, CT  
Lisa Krall, Soil Scientist, USDA-NRCS, Vernon, CT  
Michael McBride, Curator, Henry Whitfield State Museum, Connecticut Dept. of Culture and Tourism, Guilford, CT  
Yalimar Pagan, Student, UCONN Mentorship Program, Storrs, CT  
Samantha Pare, Student, UCONN Mentorship Program, Storrs, CT  
Abraham Parrish, GIS Specialist, Map Collection, Yale University, New Haven, CT  
Lee Rubin, Student, UCONN Mentorship Program, Storrs, CT  
Russell Schimner, Undergraduate, Dept. of Anthropology, Yale University, New Haven, CT  
John Spalding, Archaeologist, FOSA/ABAS, Rocky Hill, CT  
Tom Tartaron, Associate Professor, Dept. of Anthropology, Yale University, New Haven, CT  
Jim Turenne, Assistant State Soil Scientist, USDA-NRCS, Warwick, RI  
Paul Urban, Buildings & Ground Coordinator, Harriet Beecher Stowe Center, Hartford, CT  
Mary Ellen White, Manager of Marketing and Public Relations, Harriet Beecher Stowe Center, Hartford, CT

**Activities:**

All field activities were completed on 26 and 28 July 2004.

**Summary:**

1. A GEM-300 sensor (S/N 047; AG0002942797) and accessories (two batteries, battery charger, cables,

software, operation manual, carrying and shipping cases) were transferred from the National Soil Survey Center to the Connecticut Soil Staff.

2. A baseline EMI survey that showed the spatial distribution of apparent conductivity ( $EC_a$ ) across a research site was completed at the University of Connecticut's Animal-Waste Stacking Project, Mansfield, Connecticut.
3. Both ground-penetrating radar and electromagnetic induction were used over relatively large areas to acquire data that would assist archaeological site assessments. At all sites, GPR provided satisfactory penetration depths and resolution of subsurface features. Radar records collected with the 400 MHz antenna were of good interpretative quality. Two- and three-dimensional interpretations and the use of time sliced images were used to improve interpretations. At two archaeological sites, EMI provided supporting information and was used to detect buried cultural anomalies.
4. Geophysical surveys at each archaeological site revealed valuable subsurface information. While no major subsurface structures were evident in data, both EMI and GPR provided information on the location and identity of buried cultural features. Archaeological investigations and the detection of buried artifacts with GPR were hampered by the presence of numerous scattering bodies in the soil, which masked the presences of buried artifact and complicated interpretations.
5. Three-dimensional imagery did not significantly improve radar interpretations. Two-dimensional radar records require less resources and provide more immediate and often more useful information on suspected buried cultural features than did three-dimensional, processed radar images.
6. Three-dimensional imagery did provide records as to the general locations of anomalous zones in the subsurface. Studies document the need for accurate horizontal positioning and closely spaced GPR traverse lines for archaeological investigations.

It was my pleasure to work in Connecticut and to be of assistance to you.

With kind regards,

James A. Doolittle  
 Research Soil Scientist  
 National Soil Survey Center

cc:

- B. Ahrens, Director, USDA-NRCS, National Soil Survey Center, Federal Building, Room 152, 100 Centennial Mall North, Lincoln, NE 68508-3866
- N. F. Bellantoni, Connecticut State Archaeologist, Connecticut Archaeology Center, Box U-4214, University of Connecticut, Storrs, CT 06269-4214
- K. Kolesinskas, State Soil Scientist, USDA-NRCS, 344 Merrow Road, Suite A, Tolland, CT 06084-3917
- M. Golden, Director of Soils Survey Division, USDA-NRCS, Room 4250 South Building, 14th & Independence Ave. SW, Washington, DC 20250
- C. Olson, National Leader, Soil Investigation Staff, USDA-NRCS, National Soil Survey Center, Federal Building, Room 152, 100 Centennial Mall North, Lincoln, NE 68508-3866
- B. Thompson, MO Staff Leader, USDA-NRCS, 451 West Street, Amherst, MA 01002-2934
- W. Tuttle, Soil Scientist (Geophysical), USDA-NRCS-NSSC, P.O. Box 974, Federal Building, Room G08, 207 West Main Street, Wilkesboro, NC 28697

### **Equipment:**

The radar unit is the TerraSIRch Subsurface Interface Radar (SIR) System-3000 (here after referred to as the SIR System-3000), manufactured by Geophysical Survey Systems, Inc.<sup>1</sup> The SIR System-3000 consists of a digital control unit (DC-3000) with keypad, SVGA video screen, and connector panel. A 10.8-volt lithium-ion rechargeable battery powers the system. The SIR System-3000 weighs about 9 lbs (4.1 kg) and is backpack portable. With an antenna, this system requires two people to operate. A 400 MHz antenna was used in the studies described in this report. Scanning rates of 62 scans/sec and scanning times of 40 and 50 ns were used. The use and operation of GPR are discussed by Morey (1974), Doolittle (1987), and Daniels (1996).

The RADAN for Windows (version 5.0) software program developed by Geophysical Survey Systems, Inc, was used to process the radar records.<sup>1</sup> Processing included setting the initial pulse to time zero, color table and transformation selection, marker editing, distance normalization, and range gain adjustments. In addition radar records were migrated to remove hyperbola diffractions and to correct the geometry of steeply dipping layers. For each site, radar records were processed into a three-dimensional image using the 3D QuickDraw for RADAN Windows NT software developed by Geophysical Survey Systems, Inc.<sup>1</sup> Once processed, arbitrary cross sections and time slices were viewed and selected images attached to this report.

A GEM300 multifrequency sensor, developed by Geophysical Survey Systems, Inc.,<sup>1</sup> was also used. This sensor is configured to simultaneously measure up to 16 frequencies between 330 and 19,950 Hz with a fixed coil separation (1.3 m). Won and others (1996) have described the use and operation of this sensor. With the GEM300 sensor, the depth of penetration is considered “skin depth limited” rather than “geometry limited.” The skin-depth represents the maximum depth of penetration and is frequency and soil dependent: low frequency signals travel farther through conductive mediums than high frequency signal. The theoretical penetration depth of the GEM300 sensor is dependent upon the bulk conductivity of the profiled earthen material(s) and the operating frequency. Multifrequency sounding with the GEM300 sensor allows multiple depths to be profiled with one pass of the sensor.

To help summarize the results of EMI surveys, the SURFER for Windows, version 8.0, developed by Golden Software, Inc., was used to construct two-dimensional simulations.<sup>1</sup> Grids of  $EC_a$  data were created using kriging methods with an octant search.

### **Survey Procedures:**

Prior to field work, each site was walked and reviewed, and the most desirable study area(s) was selected. To expedite field work, two equal length and parallel lines were set out at each site. These two parallel lines defined a rectangular grid area. Survey flags were inserted in the ground at equal intervals along each of the two lines. For positional accuracy, surveys were completed by stretching and sequentially moving a reference line between similarly numbered flags on the two parallel grid lines.

Pulling the 400 MHz antenna along a reference line that was stretched between similarly numbered flags on the two parallel survey lines completed a GPR traverse. Along the reference line, marks were spaced at 1-m intervals. As the antenna was towed passed each reference point, a vertical mark was impressed on the radar record. At the conclusion of each traverse, the reference line was moved sequentially to the next flags on the two parallel survey lines. Walking, in a back and forth manner, along the reference line between similarly numbered flags on the two parallel survey lines completed a GPR survey.

The GEM300 sensor was held at hip height. In the continuous mode, EMI traverses were completed by walking with the GEM300 sensor in a back and forth pattern along the reference line that was stretched and sequentially moved between similarly numbered flags on the opposing set of parallel lines. In the continuous mode, measurements were recorded at 1-sec intervals. For each traverse line, the location of each measurement was later adjusted to provide a uniform interval between observation points. In the station-to station mode, the

---

<sup>1</sup> Manufacturer's names are provided for specific information; use does not constitute endorsement.

GEM300 sensor was moved to reference points spaced at 5-m intervals along the reference line. At each 5-m reference point, measurements were obtained in both the horizontal and vertical dipole orientations

### **Electromagnetic Induction:**

Electromagnetic induction is a noninvasive geophysical tool that can be used for detailed site assessments. Advantages of EMI are its portability, speed of operation, flexible observation depths, and moderate resolution of subsurface features. Electromagnetic induction can provide in a relatively short time the large number of observations that are needed to comprehensively cover sites. Maps prepared from correctly interpreted EMI data provide the basis for assessing site conditions, planning further investigations, and locating sampling or monitoring sites.

Apparent conductivity is a weighted, average conductivity measurement for a column of earthen materials to a specific depth (Greenhouse and Slaine, 1983). Variations in  $E_a$  are caused by changes in the electrical conductivity of earthen materials. Electrical conductivity is influenced by the type and concentration of ions in solution, the amount and type of clays in the soil matrix, the volumetric water content, and the temperature and phase of the soil water (McNeill, 1980). Soil  $E_a$  increases with increased soluble salts, water, and clay contents (Kachanoski et al., 1988; Rhoades et al., 1976).

Electromagnetic induction measures vertical and lateral variations in  $E_a$ . Values of  $E_a$  are seldom diagnostic in themselves, but lateral and vertical variations in these measurements can be used to infer changes in soils and soil properties. Interpretations are based on the identification of spatial patterns within data sets. To assist interpretations, computer simulations are normally used.

Two frequencies were used with the GEM-300 sensor: 9810 and 14610 Hz. These frequencies correspond to the operating frequencies of the Geonics Limited EM31 (9810 Hz) and EM38 (14610 Hz) meters. For the GEM300 sensor, the depth of penetration is considered “skin depth” limited. The “skin depth” can be estimated using the following formula (McNeill, 1996):

$$D = 500 / (s * f)^{-2} \quad [1]$$

Where  $s$  is the ground conductivity (mS/m) and  $f$  is the frequency (kHz). At the UCONN Stacking Project Site, with the GEM300 sensor held at hip height in the vertical dipole orientation,  $EC_a$  averaged 6.5 and 4.1 mS/m at frequencies of 9810, and 14610 Hz, respectively. Based on equation [1], the selected frequencies and these averaged conductivities, the estimated skin depths (penetration depths) would be about 63 m at 9,810 Hz, and 64 m at 14,610 Hz. However, these depths are hypothetical and unconfirmed by field research. While the induced magnetic fields may achieve these depths, the response from these depths is probably too weak to be sensed by the GEM300. Because of these uncertainties, it is perhaps best to view the GEM-300 sensor as being “geometry limited.” The intercoil spacing on the GEM-300 sensor is 1.3 m. Using the relationship expressed by McNeill (1980), the depth of penetration is 0.75 and 1.5 times the intercoil spacing in the horizontal and vertical dipole orientations, respectively. With the GEM-300 sensor, this relationship would provide penetration depths of about 1- and 2- m in the horizontal and vertical dipole orientations, respectively.

### **EMI Survey of University of Connecticut (UCONN) Animal-Waste Stacking Project:**

Dr. Thomas F. Morris (Assistant Professor, Plant Science Department, University of Connecticut) and his graduate student, Chris Clark, are conducting a study of alternative stacking practices. The purpose of the project is to study the effectiveness of various pads and cover materials in reducing losses from field stacked manure. The research site is presently being prepared and a background EMI survey was requested.

Electromagnetic induction has been successfully used to investigate relative concentration, extent, and movement of contaminants from waste-holding facilities (Brune and Doolittle, 1990; Drommerhausen, 1995; Eigenberg et al., 1998; Radcliffe et al., 1994; Ranjan and Karthigesu, 1995; Siegrist and Hargett, 1989; and Stierman and Ruedisili, 1988). While EMI does not provide a direct measurement of any one specific ion or

compound, measurements of  $E_a$  have been correlated with the concentration of chloride, ammonia, and nitrate nitrogen in soils (Brune and Doolittle, 1990; Ranjan and Karthigesu, 1995; Eigenberg et al., 1998).

The project is located at the UCONN Plant Science Research Facility on Storrs Road, in Mansfield. The project site is located in a grassed area of Woodbridge fine sandy loam, 3 to 8% slopes (Ilgen et al., 1966). The very deep to bedrock, moderately deep to densic material, moderately well drained Woodbridge soil forms in subglacial till on uplands. Woodbridge is a member of the coarse-loamy, mixed, active, mesic Aquic Dystrudepts family

A grid was established immediately down slope of a line of stacking plots. The maximum dimensions of the grid were 50- by 30-m. Traverse lines were either 40 or 50-m long, orientated parallel with the line of stacking pads, and spaced 5-m apart.

Table 1 summarizes the data collected with the GEM300 sensor operated in the station-to-station mode at the UCONN Stacking Project Site. Apparent conductivity was low and generally invariable across the site. With a frequency of 9810 Hz,  $EC_a$  averaged 6.7 and 6.5 mS/m in the horizontal and vertical dipole orientation, respectively. In the horizontal dipole orientation, although  $EC_a$  ranged from 4.1 to 12.3 mS/m, fifty percent of the observations had values of  $EC_a$  between 6.1 and 7.1 mS/m. In the vertical dipole orientation, although  $EC_a$  ranged from -25.4 to 11.6 mS/m, fifty percent of the observation had values of  $EC_a$  between 6.3 and 7.7 mS/m. With a frequency of 14610 Hz,  $EC_a$  averaged 3.9 and 4.1 mS/m in the horizontal and vertical dipole orientation, respectively. In the horizontal dipole orientation,  $EC_a$  ranged from 1.9 to 6.2 mS/m, with fifty percent of the observations between 3.4 and 4.4 mS/m. In the vertical dipole orientation, although  $EC_a$  ranged from -10.7 to 10.0 mS/m, fifty percent of the observation had values of  $EC_a$  between 3.6 and 4.9 mS/m.

**Table 1. Apparent Conductivity Data collected with the GEM-300 Sensor at the University of Connecticut Stacking Area Research Site. Station to Station Survey.**  
*All values are in mS/m*

	9810-V	9810-H	14610-V	14610-H
<b>Number</b>	72	72	72	72
<b>Average</b>	6.5	6.7	4.1	3.9
<b>SD</b>	4.0	1.3	2.1	0.9
<b>Minimum</b>	-25.4	4.1	-10.7	1.9
<b>Maximum</b>	11.6	12.3	10.0	6.2
<b>25%-tile</b>	6.3	6.1	3.6	3.4
<b>75%-tile</b>	7.7	7.1	4.9	4.4

Figure 1 shows the results of the EMI surveys conducted with the GEM-300 sensor in the station-to-station survey mode. Apparent conductivity is low and invariable across most of this site. Higher values of  $EC_a$  were measured in the right-hand portions of the survey area (most obvious in the lower plots; in the data collected at 9810 Hz) where existing subsurface drains breach the surface and the ground surface is lower. In this area of the grid, EMI responses are believed to reflect the presence of the pipe and water and contaminants leached from the adjoining fields.

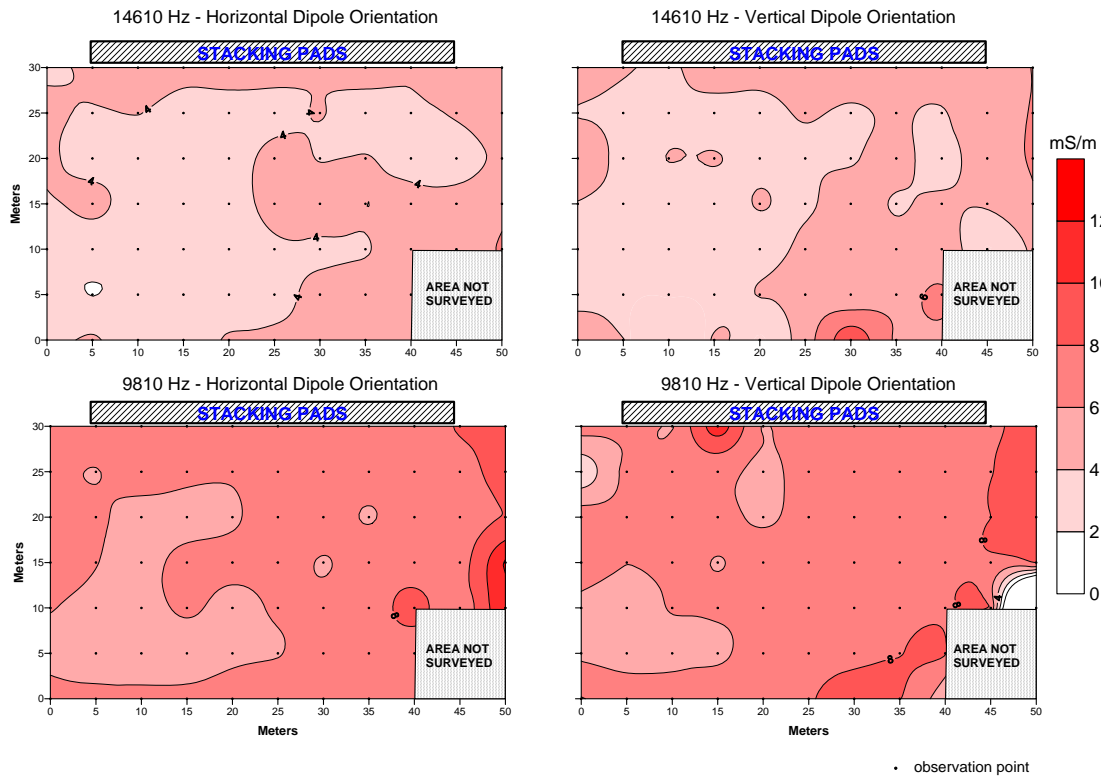


Figure 1. Results of the EMI survey at the University of Connecticut Stacking Project Site, GEM300 Sensor- Station-to-Station mode of operation.

**Table 2. Apparent Conductivity Data collected with the GEM-300 Sensor at the University of Connecticut Stacking Area Research Site. Continuous Surveys.**  
All values are in mS/m

	9810-V	9810-H	14610-V	14610-H
<b>Number</b>	516	491	516	491
<b>Average</b>	4.2	3.1	0.8	1.1
<b>SD</b>	1.4	2.3	1.2	1.5
<b>Minimum</b>	-2.3	-22.9	-4.8	-5.8
<b>Maximum</b>	15.9	12.1	6.3	11.4
<b>25%-tile</b>	3.5	1.9	0.1	0.3
<b>75%-tile</b>	4.7	3.9	1.5	1.7

Table 2 summarizes the data collected with the GEM300 sensor operated in the continuous mode at the UCONN Stacking Project Site. Apparent conductivity recorded in the continuous mode was noticeably lower than  $EC_a$  measured in the station-to-station mode. This result was unexpected and unusual. As different operators conducted each survey, differences in the height at which the meter was held and/or the presence of metallic objects on one or both the operators may account for some of the observed disparity in these measurements. In the continuous mode  $EC_a$  was low and generally invariable across the site. With a frequency of 9810 Hz,  $EC_a$  averaged 3.1 and 4.2 mS/m in the horizontal and vertical dipole orientation, respectively. In the horizontal dipole orientation, although  $EC_a$  ranged from -22.9 to 12.1 mS/m, fifty percent of the observations had values of  $EC_a$  between 1.9 and 3.9 mS/m. In the vertical dipole orientation,  $EC_a$  ranged from -2.3 to 15.9 mS/m, with fifty percent of the observations between 3.5 and 4.7 mS/m. With a frequency of 14610 Hz,  $EC_a$  averaged only 1.1 and 0.8 mS/m in the horizontal and vertical dipole orientation, respectively. In the horizontal dipole orientation,

$EC_a$  ranged from -5.8 to 11.4 mS/m, with fifty percent of the observations between 0.3 and 1.7 mS/m. In the vertical dipole orientation,  $EC_a$  ranged from -4.8 to 6.3 mS/m, with fifty percent of the observations between 0.1 and 1.5 mS/m.

Figure 2 shows the results of the EMI surveys conducted with the GEM-300 sensor in the continuous survey mode. High values of  $EC_a$  were recorded in the right-hand portion of the survey area near the point where a subsurface drainage pipe breaches the surface. The effects of very resistive soils and the possibilities of equipment and/or operator errors may be responsible for the dissimilarities in  $EC_a$  and spatial patterns evident in figures 1 and 2.

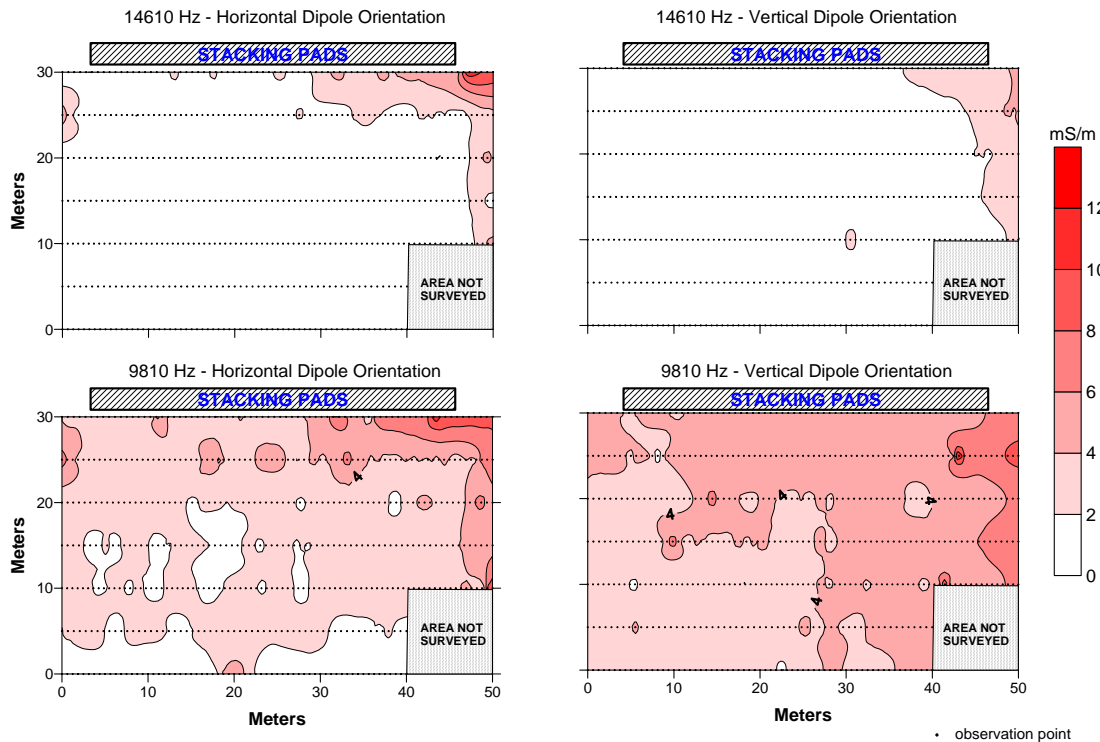


Figure 2. Results of the EMI survey at the University of Connecticut Stacking Project Site, GEM300 Sensor-Continuous mode of operation.

### *ARCHAEOLOGICAL INVESTIGATIONS:*

#### **EMI and Archaeological Investigations:**

Electromagnetic induction has been used to detect subsurface anomalies of potential archaeological significance. Although EMI lacks the resolution of GPR, it can be used in almost any soil or earthen material. Results depend upon the degree of contrast between a buried cultural feature and the soil materials. Electromagnetic induction has been used to locate air-filled voids in tombs (Frohlich and Lancaster, 1986), and delineate anthropogenically modified soil of mounds (Dalan, 1990).

#### **Ground-Penetrating Radar and Archaeological Investigations:**

A favorable feature of GPR for archaeological investigations is its ability to detect disturbances and the intrusion of foreign materials in soils. In many soils, GPR is a useful tool for locating burials (Bevan, 1991; Gracia et al., 2000; King et al., 1993; and Vaughan, 1986). However, results vary with soils. In some soils, rates of signal attenuation are so severe that GPR cannot provide satisfactory profiling depths. Even under favorable site conditions (i.e. dry, coarse-textured soils) the detection of a burial is never assured with GPR. The detection of burials is affected by (1) the electromagnetic gradient existing between the feature and the soil, (2) the size, depth, and shape of the buried feature, and (3) the presence of scattering bodies within the soil (Vickers et al., 1976).

The amount of energy reflected back to an antenna by a buried object is a function of the contrast in dielectric properties that exists between an object and the surrounding soil. The greater and more abrupt the difference in dielectric properties, the greater the amount of energy that is reflected back to an antenna, and the more intense will be the amplitude of the reflected signals on the radar record. The reflection coefficient of a subsurface interface is dependent on the difference in dielectric permittivity ( $E_r$ ) that exists between the two materials. As the  $E_r$  of a material is strongly dependent upon its moisture content, the amount of energy reflected back from an interface is dependent on the abruptness and contrast in moisture contents of the materials. At first, most buried objects generally contrast with the surrounding soil matrix. However, with the passage of time, buried objects decay or weather and become less electrically contrasting with the soil.

The size and depth of a burial affect detection. Large objects reflect more energy and are easier to detect than small objects. The reflective power of a buried object decreases with the fourth power of the distance to the object (Bevan and Kenyon, 1975). Most bones are too small to be distinguished with GPR (Bevan, 1991; Killam, 1990). Bevan (1991) noted that it is more likely that GPR will detect the disturbed soil within a grave shaft, a partially or totally intact coffin, or the chemically altered soil materials that directly surrounds a burial rather than the bones themselves. However, in soils that lack contrasting soil horizons or geologic strata, the detection of soil disturbances or grave shafts is more difficult. In addition, with the passage of time, natural soil-forming processes erase the signs of disturbances.

Burials are difficult to distinguish in soils having numerous rock fragments, tree roots, animal burrows, modern cultural features, or highly stratified or segmented horizons or layers. These scattering bodies produce undesired subsurface reflections that complicate radar records. Under adverse conditions, "desired" cultural features are indistinguishable from the background clutter. In soils having numerous scattering bodies, GPR often provide little meaningful information to supplement traditional sampling methods (Bruzewicz et al., 1986). The identification of buried cultural features was complicated by scattering bodies in radar surveys conducted by Bevan (1991), Dolphin and Yetter (1985), Doolittle (1988), and Vaughan (1986).

On radar records, the depth, shape, size, and location of subsurface features may be used as clues to infer buried cultural features. In the past, reflections were identified and correlated on two-dimensional radar records. Today, three-dimensional imaging techniques can be used to distinguish coherent noise components, reduce interpretation uncertainties, and aid identification of potential targets (Pipan et al., 1999). Three-dimensional interpretations of GPR data have been used to identify burials, middens, and other cultural features (Conyers and Goodman, 1997; Whiting et al., 2000; Goodman et al., 2004). In the past, the use of 3-D images was restricted because of the use of analog signals and the lack of satisfactory signal-processing software. The

recent development of sophisticated signal-processing software has enabled signal enhancement and improved pattern-recognition on some radar records.

In recent years, a sophisticated type of GPR data manipulation, known as *amplitude slice-map analysis*, has been used in archaeological investigations (Conyers and Goodman, 1997). A 3-D image of a site is derived from the computer analysis of a series of closely-spaced, two-dimensional radar records (Conyers and Goodman, 1997). Amplitude differences within the 3-D image are analyzed in "time-slices" that examine only changes within specific depths in the ground (Conyers and Goodman, 1997). Time-slice data are created using spatially averaged amplitudes of return reflections. The reflected energy is averaged horizontally between each set of parallel radar records and in specified time windows to create a time-slice. Each amplitude time-slice shows the spatial distribution of reflected wave amplitudes, which are indicative of changes in soil properties or the presence of buried features.

#### *Whitfield House, Guilford, Connecticut:*

Begun in 1639, the Henry Whitfield House, which is located in Guilford, Connecticut, is the oldest remaining house in Connecticut. The Old Stone House was the home of Guilford's first minister, Henry Whitfield, and also served as a defensive stronghold for the community. A GPR survey was conducted to ascertain whether any outbuildings occur in the open areas to the northwest and southeast of the house. The study areas are located in an area that has been mapped as Paxton fine sandy loam, 3 to 8 percent slopes (Reynolds, 1979). An examination of the soils revealed the dominance of Cheshire or Hartford soils in the surveyed areas. The very deep, well drained Cheshire soil formed in supraglacial till on uplands. Cheshire is a member of the coarse-loamy, mixed, semiactive, mesic Typic Dystrudepts family. The very deep, somewhat excessively drained Hartford soil formed in sandy glacial outwash. Hartford is a member of the sandy, mixed, mesic Typic Dystrudepts family.

#### Survey Procedures:

Two grids were established in grassed areas surrounding the Whitfield House. A 25- by 23-m grid, consisting of 48 survey lines, was laid out across an open area to the northwest of the house. This grid area will be referred to as *Area A*. The origin of the grid was located in the northwest corner of the surveyed area. Survey lines were 25-m long, orientated in an essentially north northwest to south southeast direction, and spaced 50 cm apart. Also, a 10 by 30-m grid, consisting of 31 survey lines, was laid out across an open area to the southeast of the house. This grid area will be referred to as *Area B*. The origin of the grid was located in the southwest corner of the surveyed area. Survey lines were 10-m long, orientated in an essentially west-southwest to east-northeast direction, and spaced 100 cm apart. Ground-penetrating radar surveys were completed in both areas. An EMI survey was completed in Area B.

Based on hyperbola-matching processing techniques (the shape of a hyperbole is dependent on signal velocity), the velocity of propagation decreased with depth, but over the scanned depth averaged about 0.09 m/ns ( $E_r$  of 11). With a scanning time of 40 ns, the maximum penetration depth was about 1.8 m.

#### Results:

##### *Area A*

Figure 3 is a representative radar record from Area A. The short, white, vertical lines at the top of the radar record represent equally spaced (1-m) reference points along the radar traverse. The vertical scale along the left-hand margin of this figure is a depth scale (in meters) that is based on an averaged velocity of pulse propagation of 0.09 m/ns. Note that the depth scale in Figure 3 is exaggerated relative to the horizontal scale.

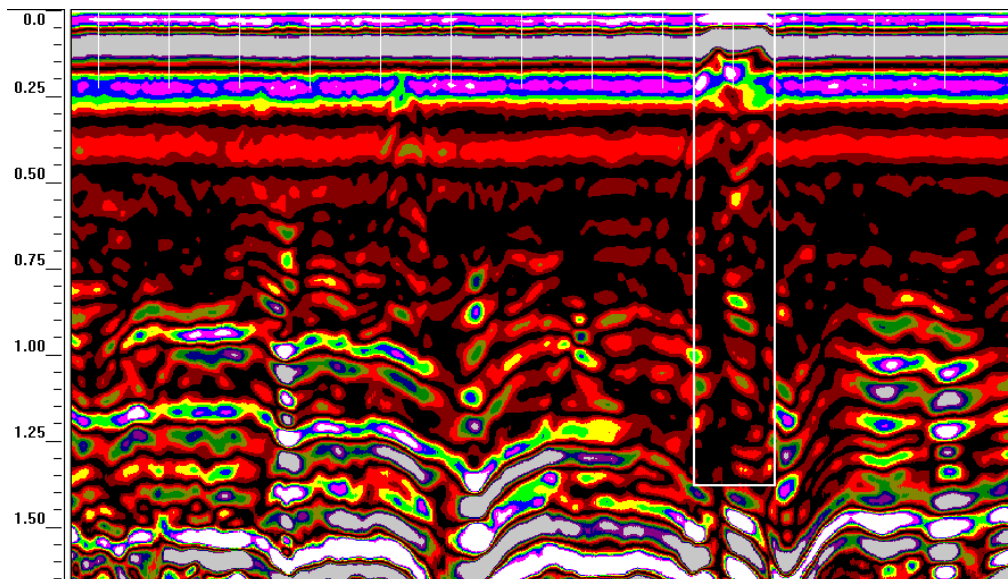


*Figure 3. A refilled soil pit is shown on this radar record from Area A at the Whitfield House.*

In Figure 3, the location of the refilled soil pit is enclosed in a rectangle. The refilled pit was covered with a piece of plywood that provides a noticeably higher amplitude signal which aids interpretation. The sides of the refilled shaft are essentially invisible. The refilled soil materials provide some reflections whose patterns contrast with the bounding undisturbed soil materials. The refilled soil materials are indicated by hyperbolas starting near the surface with some ringing in time (depth). The dominance of planar reflectors in the lower part of the radar record supports water resorting of glacial materials and the presence of Hartford soil in the grid area.

Figure 4 contains four time-slice images of Area A. In Figure 4, all distance units are expressed in meters. The origin is located in the lower left-hand corner (northwest corner of grid area) of each slice. The four horizontal “time-slices” represent depths of about 0, 50, 100, and 150 cm. These depths were based on an averaged signal propagation velocity of 0.09 m/ns through the soil. The width of the time-slice is about 20 cm. The dark vertical lines along the north (left) and south (right) boundaries of each time-slice image are artifacts of the processing techniques used.

In Figure 4, the shallowest (0 cm) slice reveals amplitude patterns that are associated with slight differences in soil moisture and soil density. Amplitudes shown on the surface slice are very low with the exception of two short linear patterns in the lower part of the slice. One of these reflections (“A” at X = 15.5 to 16.5 m; Y = 0.5 to 2.5 m) represents a refilled soil pit with a plywood sheet cover. The identity of the other linear reflector is unknown. In the 50 cm slice, two areas of higher amplitude (black) features can be identified in the northeast and southeast corners of the site (in Figure 4, see “A” and “B” on the 50 cm slice). These are believed to represent the roots of nearby trees and shrubs. Other portions of this slice contain low to moderate amplitude reflections and are nondescript, though with a little imagination some faint spatial patterns can be envisioned. In the 100 cm slice, high amplitude reflections become more numerous and widespread, with a noticeable concentration near “A” in the east-central portion of the survey area. This area may be worthy of further investigations by archaeologists. The 150 cm slice contains an abundance of higher amplitude reflections that are believed to represent cobbles and dissimilar stratigraphic layers in the underlying outwash deposits.

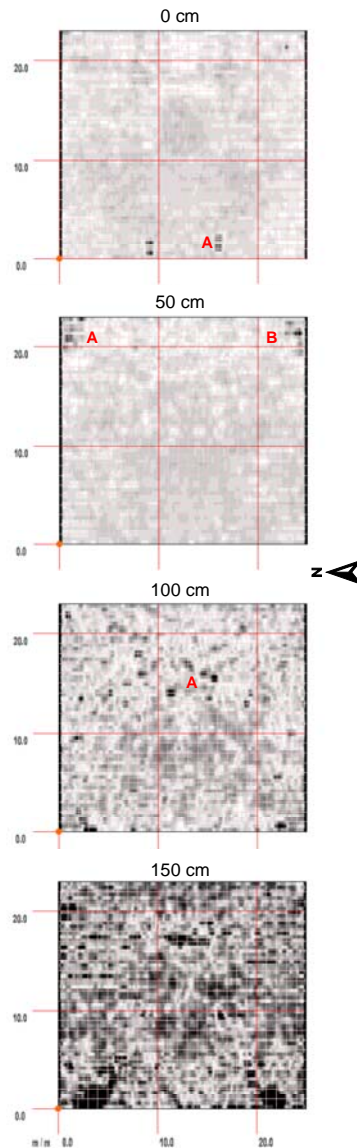
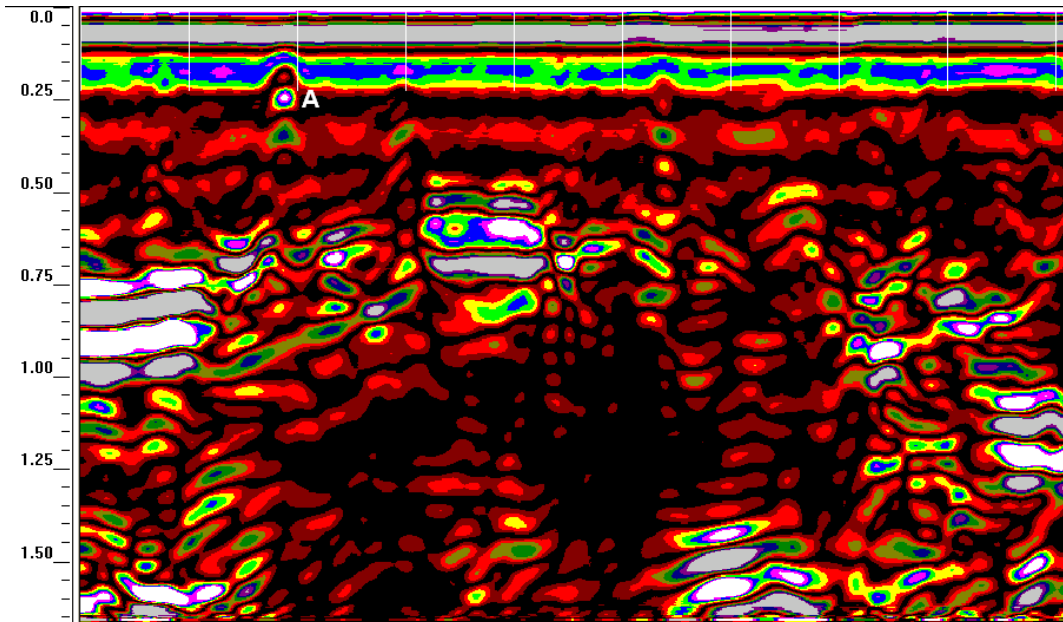


Figure 4. Time-sliced images of Area A at the Whitfield House

#### Area B GPR

Figure 5 is a representative radar record from the Area B at the Whitfield House. This radar record is from the first traverse line, which was located nearest to Stone House Lane (the line parallels the road) and in the lowest portion of the grid area. The short, white, vertical lines at the top of the radar record represent the equally spaced (1-m) reference points along the radar traverse. The vertical scale along the left-hand margin of this figure is a depth scale (in meters) that is based on a velocity of pulse propagation of 0.09 m/ns. Note that the depth scale in Figure 5 is exaggerated relative to the horizontal scale.

The radar record shown in Figure 5 is rather complex. In the first six meters (from left) multiple, inclined parallel planar reflectors suggest water reworked materials. Many of the point anomalies on the radar record are believed to represent larger coarse fragments which are common in glacial materials. The strong reflector near “A” may represent a buried artifact, rock fragment, tree root, or animal burrow. From about the six meter mark until the right-hand margin of this figure, reflections appear more chaotic suggesting disturbed materials. No clear indication of the presence of a subsurface structure is evident



*Figure 5. A radar record from Area B at the Whitfield House.*

Figure 6 contains four time-slice images of Area B. In Figure 6, all distance units are expressed in meters. The origin is located in the upper left-hand corner (southwest corner of grid area) of each slice. Stone House Lane parallels the left-hand margin of each slice. The four horizontal “time-slices” represent depths of about 0, 50, 100, and 150 cm. These depths are based on an averaged signal propagation velocity of 0.09 m/ns through the soil. The width of the time-slice is about 25 cm. The dark vertical lines along the west (upper) and east (lower) boundaries of each time-slice image are artifacts of the processing techniques used.

In Figure 6, the shallowest (0 cm) slice reveals patterns related principally to slight differences in soil moisture and density. Changes in these properties are reflected in signals of low and moderate amplitudes. In the 50 cm slice, two linear stripes of higher amplitudes can be identified extending into the grid area near the southwest corner. These are believed to represent strata shown in the left-hand portion of Figure 5. Other portions of this slice have low to moderate amplitude reflections and are nondescript. In the 100 cm and 150 cm slice, high amplitude reflections become more widespread and apparent with noticeable concentration in the central and southeast portions of the survey area. While some of these patterns are linear and therefore suggest artificial features, no clear interpretation is possible at this time.

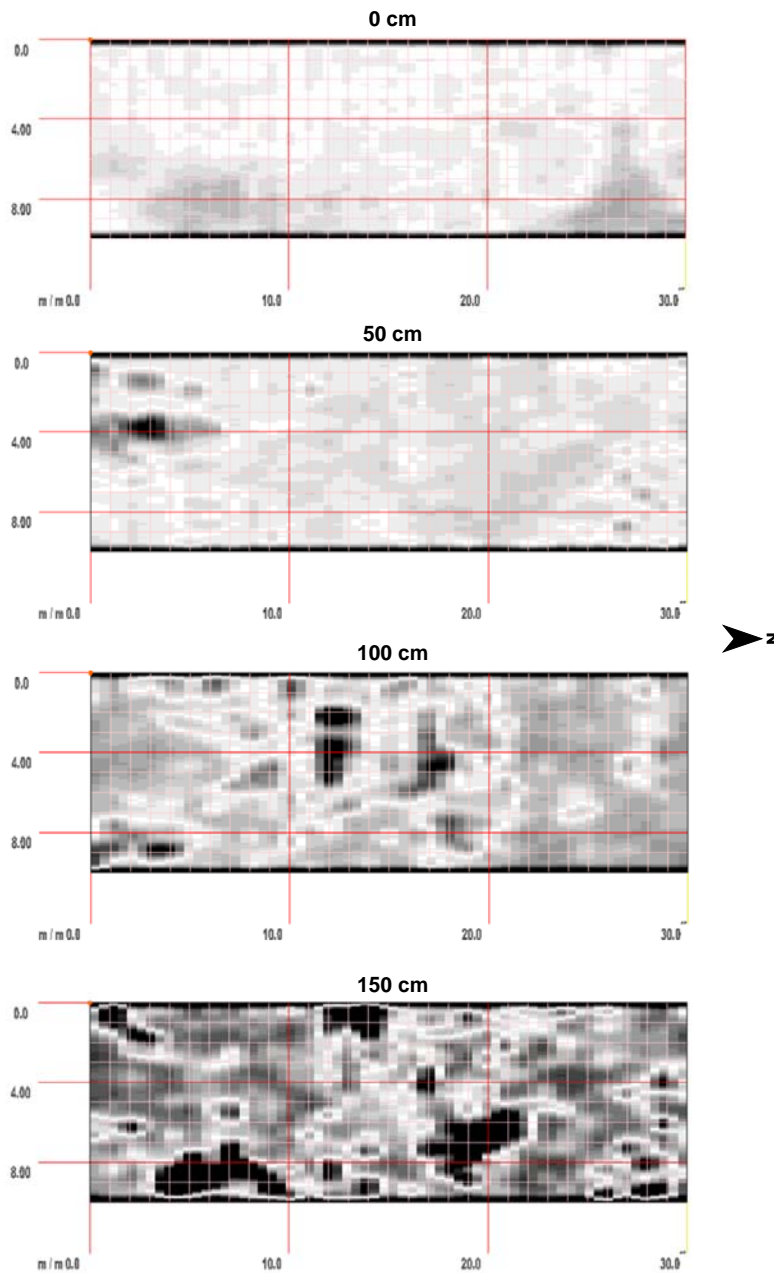


Figure 6. Time-sliced images of Area B at the Whitfield House

#### EMI Survey:

Table 3 summarizes the data collected with the GEM300 sensor operated in the vertical dipole orientation within Area B. Data were collected in the continuous mode. Within this grid,  $EC_a$  was generally low, but variable across the site. With a frequency of 9810 Hz,  $EC_a$  averaged 14.2 mS/m and ranged from -98.2 to 56.0 mS/m. One half of the observations had values of  $EC_a$  between 9.0 and 17.4 mS/m. With a frequency of 14610 Hz,  $EC_a$  averaged 12.0 mS/m and ranged from -73.3 to 46.1 mS/m. One half of the observations had values of  $EC_a$  between 7.5 and 14.9 mS/m.

**Table 3. Apparent Conductivity Data collected with the GEM-300 sensor in the vertical dipole orientation in Survey Area B at the Whitfield House.**

*(All measurements are in mS/m)*

	9810 Hz	14610 Hz
<b>Average</b>	14.2	12.0
<b>Standard Deviation</b>	10.3	8.8
<b>Minimum</b>	-98.2	-73.3
<b>Maximum</b>	56.0	46.1
<b>25% Quartile</b>	9.0	7.5
<b>75% Quartile</b>	17.4	14.9

Figure 7 is a choropleth map that shows the spatial distribution of  $EC_a$  obtained with the GEM300 sensor. In Figure 7, color variations have been used to help show the distribution of  $EC_a$ . The color interval is 1 mS/m. The locations of traverse lines and observation points (blue dots) are shown in the left-hand plot. Stone House Lane parallels the lower boundary of these plots.

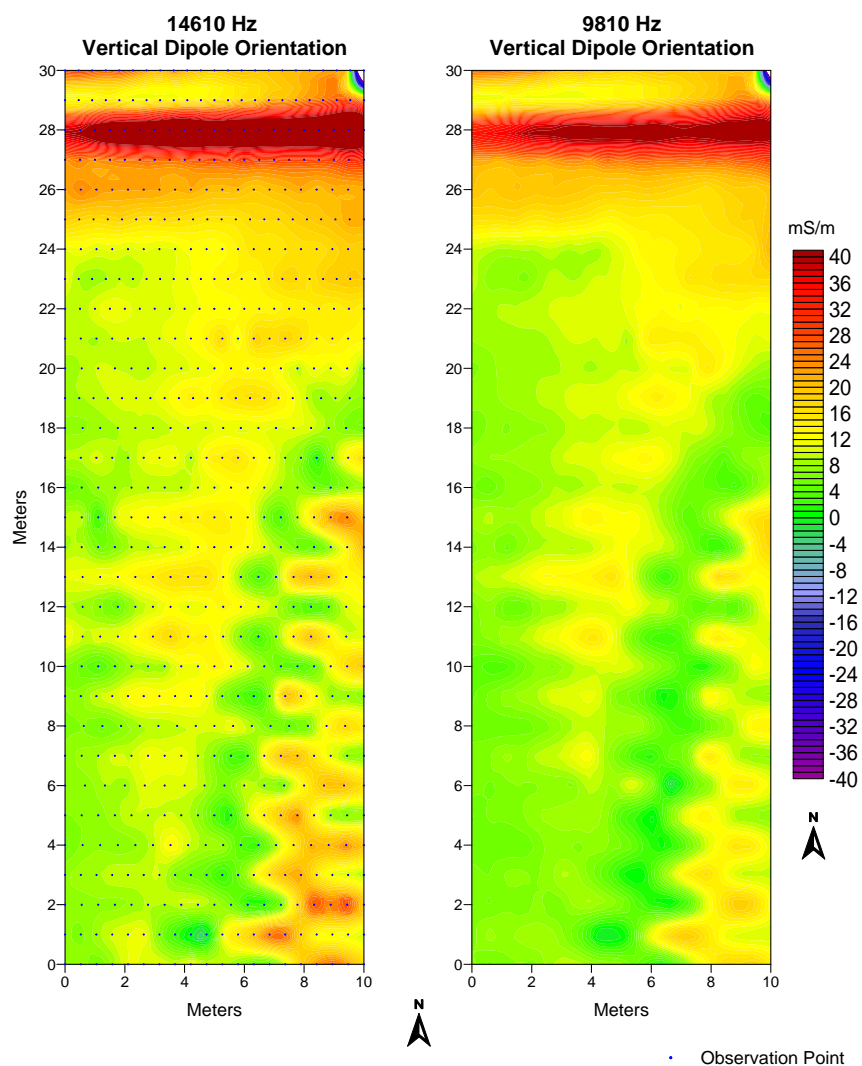


*Figure 7. Spatial distribution of apparent conductivity across Area B at the Whitfield House.*

The response from a buried utility line is evident across the upper part of each plot shown in Figure 7. Here, a line of elevated  $EC_a$  parallels the X axis of both plots. A buried metallic feature is believed to be responsible for the negative anomaly evident in the extreme northeast corner of each plot. Because of the distance between the transmitting and receiving coils and the time delay in data logging, slight spatial discrepancies exist in EMI data. These offsets and delays, as well as the gridding methods and contour intervals used in computer simulations, are responsible for the “herringbone” patterns that occur in the plots shown in Figure 7. Note how the spatial patterns form rows of parallel lines which are offset in opposite directions. This effect is most evident in detailed grids of small areas. In each plot, two linear patterns of higher  $EC_a$  appear to stretch across the plots from top to bottom.

### **Glastonbury Green Cemetery, Glastonbury, Connecticut:**

Two sections of the Glastonbury Green Cemetery were surveyed in an attempt to locate a purported unmarked grave. The cemetery is located in Glastonbury, at the intersection of Main and Hubbard streets. The cemetery is located in an area that has been mapped as Windsor loamy fine sand, 0 to 3 percent slopes (Shearin and Hill, 1962). The very deep, excessively drained Windsor soil formed in sandy glacial outwash on glaciofluvial landforms. Windsor is a member of the mixed, mesic Typic Udipsamments family.

#### Survey Procedures:

A *wildcat* survey was conducted across a family plot with three headstones. This survey was conducted to confirm the presence of two burials and to calibrate the GPR. The radar detected three burials (in all probability, buried coffins), while cemetery records showed only two burials within the site. A grid, consisting of 6 survey lines was laid out across a vacant area in the northern part of the cemetery along a cemetery road. This area was suspected to contain unmarked graves. The dimensions of the grid were 25- by 5-m. The origin of the grid was located in the southwest corner of the suspected area. The x-axis extended in a southwest to northeast trending direction along the north side of a cemetery road. Survey lines were 25 m long and spaced 100 cm apart. Along each line, reference marks were spaced at 1-m intervals.

Based on hyperbola matching techniques, the velocity of propagation decreased with depth, but over the scanned depth averaged an estimated 0.09 m/ns ( $E_r$  of 10). With a scanning time of 40 ns, the maximum penetration depth was about 1.9 m.

#### Results

Figure 8 is a radar record from the grid within the Glastonbury Green Cemetery. The radar record contains several prominent point anomalies, which are easily identifiable by their characteristic hyperbolic pattern ( $\wedge$ ). In Figure 8, several of these anomalies have been labeled with the letter “A” immediately to their right. These anomalies may represent soil strata, large rock fragments, tree roots, animal borrows, and/or buried artifacts. However, without ground-truth verifications, the identity of these anomalies remains speculative. One unmarked anomaly occurs at the base of a filled depression (see “B”). The upper part of the radar record contains several inclined and wavy reflectors that suggest disturbance and the presence of fill materials.

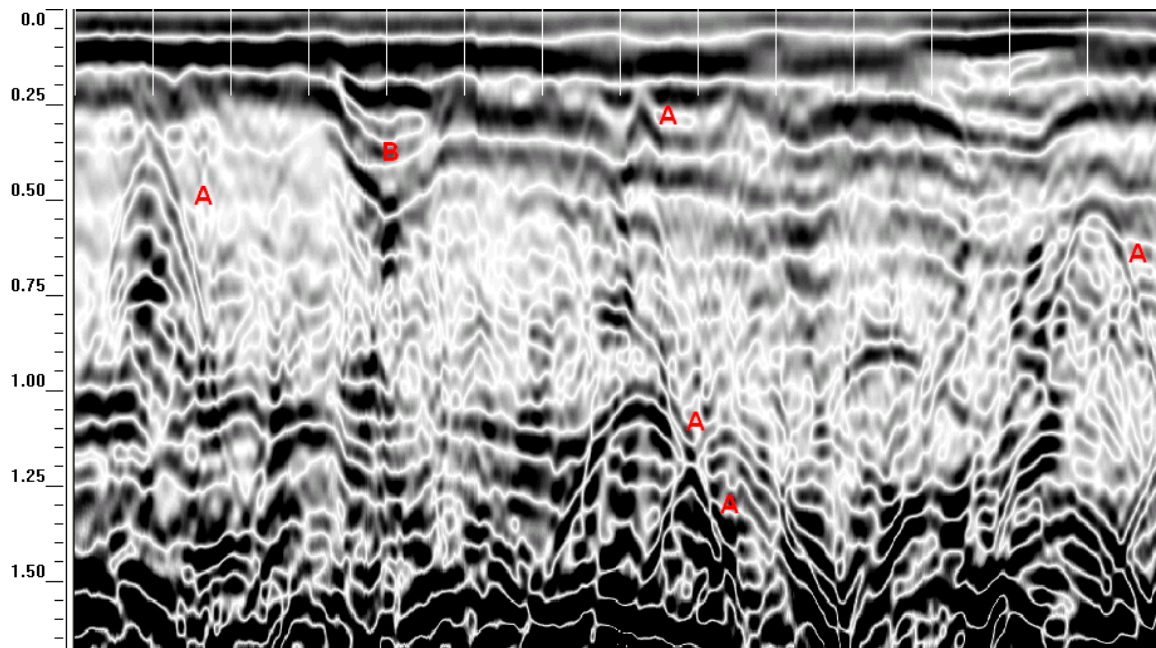


*Figure 8. Radar record from the grid area within Glastonbury Green Cemetery.*

Figure 9 contains four time-slice images of the grid area within the Glastonbury Green Cemetery. In Figure 9, all measurements are expressed in meters. The origin is located in the lower left-hand corner (southwest corner of grid area) of each slice. The four horizontal “time-slices” represent depths of about 0, 50, 100, and 150 cm. These depths were based on an averaged propagation velocity of 0.09 m/ns through the soil. The width of the time-slice is about 20 cm. The dark vertical lines along the left- and right-hand boundaries of each time-slice image are artifacts of the processing techniques used.

In Figure 9, the shallowest (0 cm) slice reveals signals of low and moderate amplitudes. The noticeable linear feature in the central part of this slice may represent fill materials or soil materials of slightly different moisture content and/or density. In the 50 cm slice, several high amplitude, linear features can be identified extending in a northwest to southeast direction in the eastern (right-hand) portion of the grid area. These features appear to have the appropriate dimensions of coffins, but are too shallow and believed to represent stratigraphic features. In the 100 cm slice, the number of high amplitude reflections increases. One of the high amplitude linear features seen in the 50 cm slice appears to persist along lines  $X = 22$  and  $Y = 1$  to 4 in the 100 cm slice. Other high amplitude reflections seen on the 100 cm slice are long, linear and variable in amplitudes. Their appearance suggests stratigraphic features in the Windsor soil. The 150 cm slice contains an abundance of high amplitude reflections, which are believed to represent strata in the Windsor soil. In the eastern (right-hand) portion of the grid, several aligned and conspicuously high amplitude linear reflectors attract some interest. Though believed to be soil strata, ground-truth auger observations may be considered to confirm this interpretation.

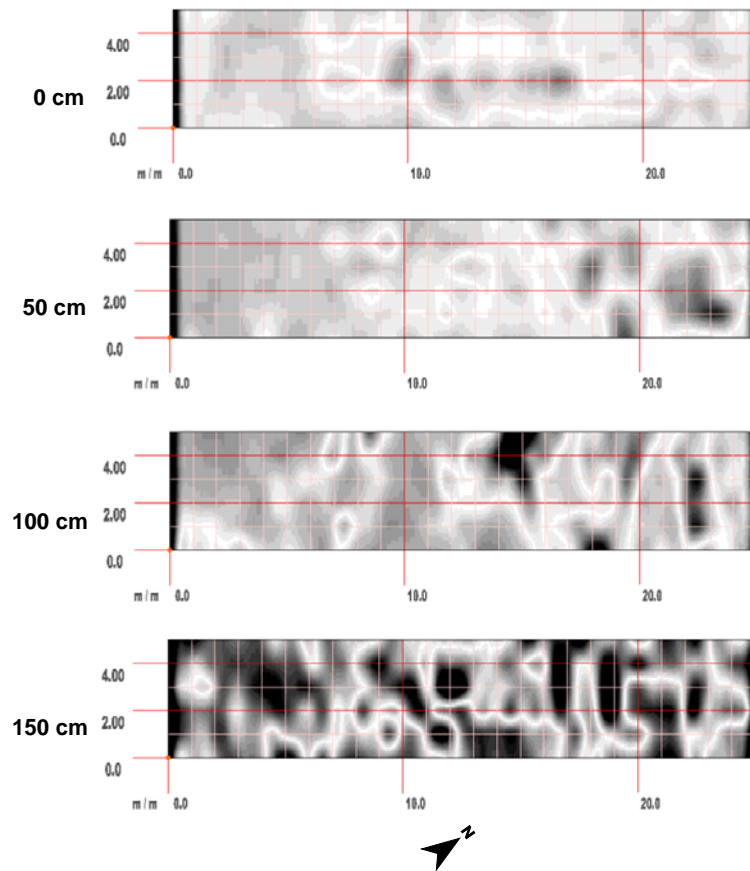


Figure 9. Time-sliced images of the grid area within the Glastonbury Green Cemetery

### **Goeffe House, Meriden:**

Ground-penetrating radar and EMI surveys were conducted in an area to the immediate south and east of the Goeffe House in an attempt to uncover evidence of outbuildings. The Goeffe House is located along North Colony Road, in Meriden, Connecticut. The house was built in 1711 by Solomon Goeffe. The study site is located in an area that has been mapped as Holyoke silt loam, rocky, 3 to 15 percent slopes (Shearin and Hill, 1962). The shallow, well drained and somewhat excessively drained Holyoke soil formed in a thin mantle of till derived mainly from basalt and red sandstone, conglomerate, and shale. Holyoke is a member of the loamy, mixed, superactive, mesic Lithic Dystrudepts family. While Holyoke soil is present in nearby areas, the survey area is located in areas of deeper Cheshire soil or disturbed urban lands (Kip Kolesinskas, personal observation).

### Survey Procedures:

An irregularly-shaped, rectangular grid was laid out across the lawn to the immediate south and east of the Goeffe House. The maximum dimensions of this grid were 33- by 17-m. The origin of the grid was located in the extreme southeast corner of the survey area. North Colony Avenue parallels the western border of the survey area at a distance of about 3 m. Three end lines were needed to define the grid area. These lines were orientated in an east-west direction, and spaced 11 and 22 m apart (having X axis coordinates of 0-, 11-, and 33-m). Electromagnetic induction and GPR surveys were conducted along parallel, north-south trending lines that were spaced 1 m apart. The GPR survey was confined to the rectangular area (X = 0- to 11-m, Y = 0- to 17-m) located in the southern portion of the site.

An EMI survey was conducted with the GEM300 sensor operated in the continuous mode, vertical dipole orientation, and at frequencies of 9810 and 14610 Hz. Brief GPR calibration trials were conducted with 400 MHz antenna. The soil was moist at the time of this investigation. Based on hyperbola matching techniques,

the velocity of propagation decreased with increasing depth, but over the scanned depth averaged 0.091 m/ns ( $E_r$  of 10.8). With a scanning time of 40 ns, the maximum penetration depth was about 1.8-m.

### Results:

#### EMI Survey

Figure 7 is a choropleth map that shows the spatial distribution of  $EC_a$  obtained with the GEM300 sensor. In Figure 7, color variations have been used to help show the distribution of  $EC_a$ . The color interval is 1 mS/m. The locations of traverse lines and observation points (red dots) are shown in the upper plot. In each plot, an area containing several  $EC_a$  anomalies is evident to the immediate south of the Goffe House. These atypical positive and negative values suggest buried metallic artifacts.

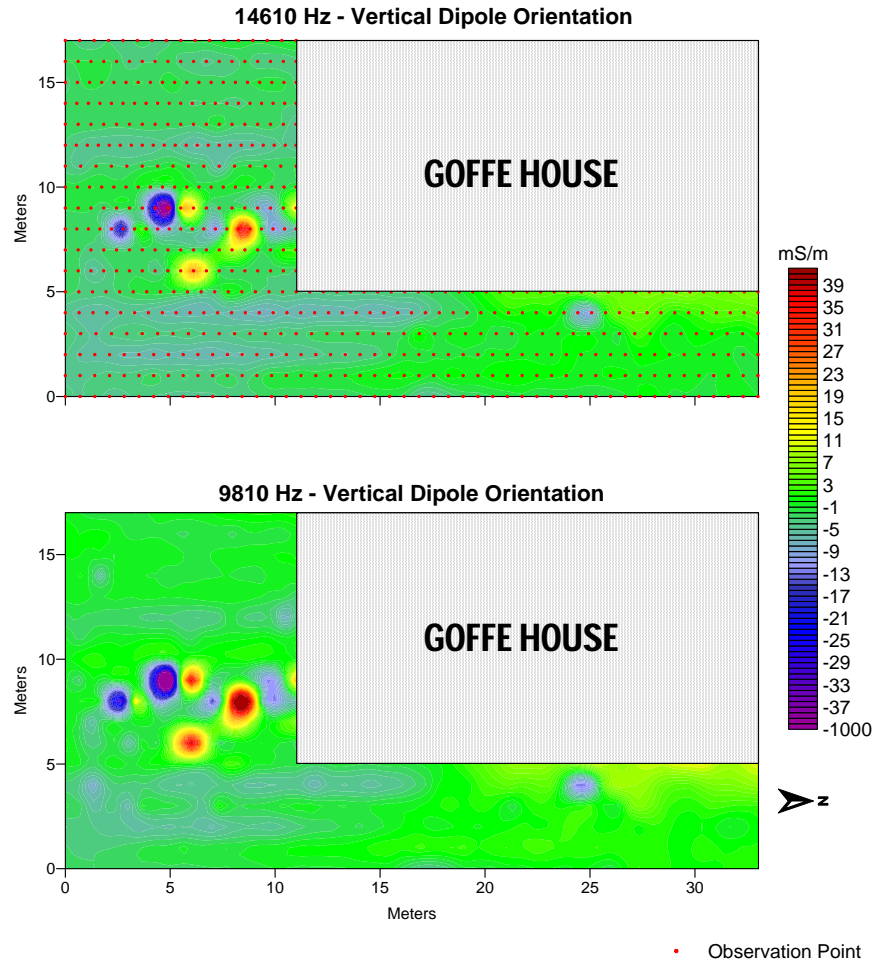
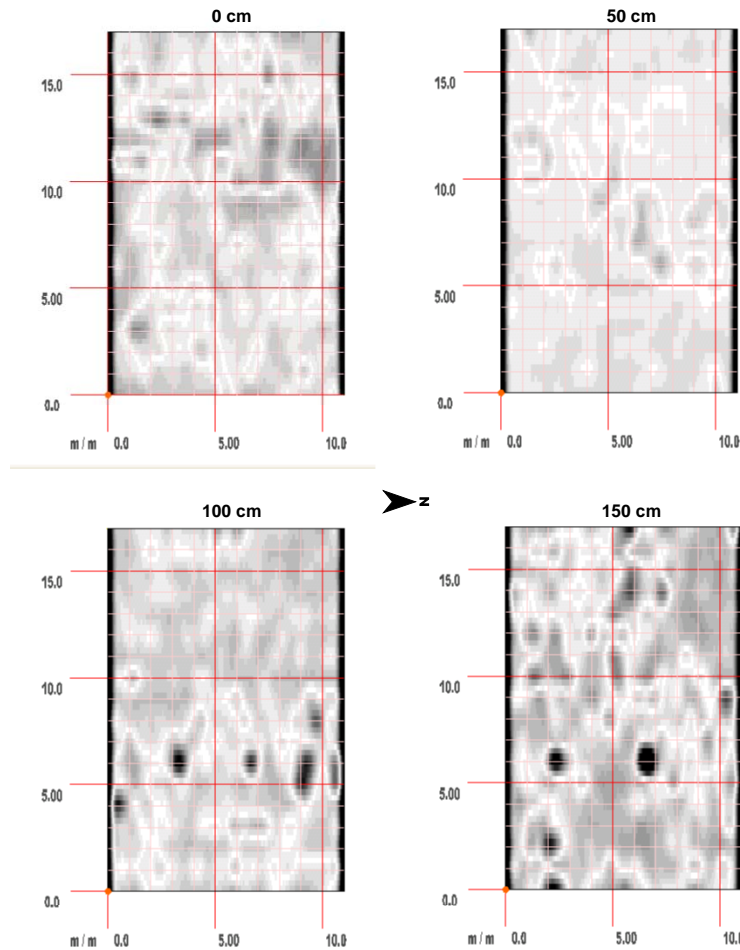


Figure 10. GEM-300 Sensor Survey at the Goffe House

Table 4 summarizes the data collected with the GEM300 sensor. The sensor recorded 525 observations. Apparent conductivity was very low and largely invariable across most of the survey area. With a frequency of 9810 Hz,  $EC_a$  averaged only -0.26 mS/m and ranged from -84.6 to 68.2 mS/m. One half of the observations had an  $EC_a$  between -2.1 and 0.9 mS/m. With a frequency of 14610 Hz,  $EC_a$  averaged -2.05 mS/m and ranged from -66.6 to 38.9 mS/m. One half of the observations had an  $EC_a$  between -3.6 and -0.8 mS/m. The very low and negative  $EC_a$  was attributed to the noticeable amounts of iron oxides ( $FeO_3$ ) in the Cheshire-like soil. Cheshire forms in Triassic materials and has horizons with color hues of 10R to 5YR.

**Table 3. Apparent Conductivity Data collected with the GEM-300 sensor in the vertical dipole orientation in Survey Area B at the Whitfield House.**  
(All measurements are in mS/m)

	9810 Hz	14610 Hz
<b>Average</b>	-0.26	-2.05
<b>Standard Deviation</b>	7.4	5.5
<b>Minimum</b>	-84.6	-66.6
<b>Maximum</b>	68.2	38.9
<b>25% Quartile</b>	-2.1	-3.6
<b>75% Quartile</b>	0.9	-0.8



*Figure 11. Time-sliced images of the GPR grid area at the Goeffe House*

Figure 11 contains four time-slice images of the area surveyed at the Goeffe House. In each diagram, the vertical width of the slice is about 13 cm. The dark vertical lines along the south (left) and north (right) boundaries of each time-slice image are artifacts of the processing techniques used.

In Figure 11, no high amplitude reflections are apparent on the time-slices until depths of 100 and 150 cm. Low and moderate amplitudes at shallow depths suggest the presences of fairly similar soil materials that lack contrasting buried or surficial cultural objects. Several high amplitude point reflectors are evident at depths of 100 and 150 cm. At both depths, a persistent, high amplitude point anomaly occurs between positions X = 6-

7-m, and Y = 5.5- to 6.5-m. Another persistent, high amplitude point anomaly occurs between positions X = 3- to 4-m, Y = 5.5- to 7-m on the 100 cm slice, and between positions X = 2- to 3-m, Y = 5.5- to 6.5-m on the 150 cm slice. Change in the horizontal position of this reflector with variations in depth indicates an inclined reflector. In addition to these features, other high amplitude point reflectors are evident in the 100 and 150 cm slices. The general location of some of these features closely approximates the location of the anomalies detected with EMI and shown in Figure 10.

### Harriet Beecher Stowe House:

The house and the surrounding grounds were purchased in 1873 by Harriet Beecher Stowe, the author of *Uncle Tom's Cabin*. Harriet Beecher Stowe lived in the house with her husband until her death in 1896. The property adjoined the property once owned by Mark Twain. The Harriet Beecher Stowe house is surrounded by Victorian era gardens.

A 23- by 50-m grid was established across the relatively open lawn area in front of the Reception Center and between the Harriet Beecher Stowe and Mark Twain houses. The long axis extended from the Reception Area towards Farmington Avenue. Large clumps of trees and shrubs necessitated dividing the grid area into two sections: Grid 1 (nearest to Reception Center) was 23- by 25-m and Grid 2 was 23- by 12-m. The two grids were separated by a 23- by 13-m area that contained the clumps of trees and shrubs.

The Soil Survey of Connecticut shows the property as being mapped as Udorthents-urban land complex. Debbie Frigon found that the materials in this area had been recognized as lake-bottom deposits of Glacial Lake Hitchcock (geology map of the Hartford North Quadrangle). These deposits consist of varved clay and silt that have an average thickness of about 20 feet.

### Grid 1

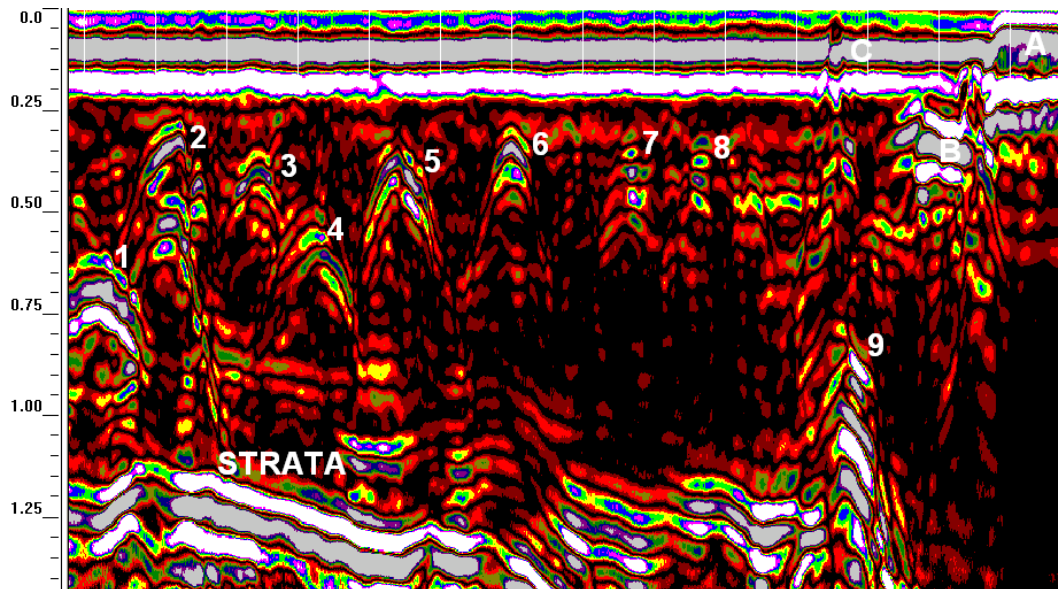


Figure 12. Radar record from Grid 1 at the Harriet Beecher House.

Figure 12 is a radar record from Grid 1. The radar record contains several prominent point anomalies, which are easily identifiable by their characteristic hyperbolic pattern ( $\wedge$ ). Several of the more prominent anomalies have been identified with numbers to their immediately right. While the identities of these anomalies are unknown, their amplitudes and seeming orderly confinement to depths of about 30- to 60-cm suggests buried artifacts. The most deeply buried anomaly (#9) appears to be overlain by a narrow shaft of disturbed and truncated soil

materials. These features suggest a refilled pit or trench. In the extreme right-hand portion of the radar record, the effects of pavement are evident at “A.” The pavement provides a denser more contrasting interface than the soil surface. As a consequence, the reflected signals have higher amplitudes, and because the propagation velocity is greater through the asphalt, the reflected signals appear to rise on the radar record. Two conspicuous reflections are evident in the near surface at “B” and “C”. The high amplitude, planar reflectors in the lower part of the radar record probably represents strata of contrasting clays and silts associated with the underlying glacio-lacustrine materials from Glacial Lake Hitchcock.

Figure 13 contains four time-slice images of Grid 1. In Figure 13, all measurements are expressed in meters. The origin is located in the lower left-hand corner (southwest corner of grid) of each slice. The four horizontal “time-slices” represent depths of about 0, 50, 100, and 150 cm. These depths were based on an averaged signal propagation velocity of 0.10 m/ns through the soil. The width of the time-slice is about 12 cm. The dark vertical lines along the west (left) and east (right) boundaries of each time-slice image are artifacts of the processing techniques used.

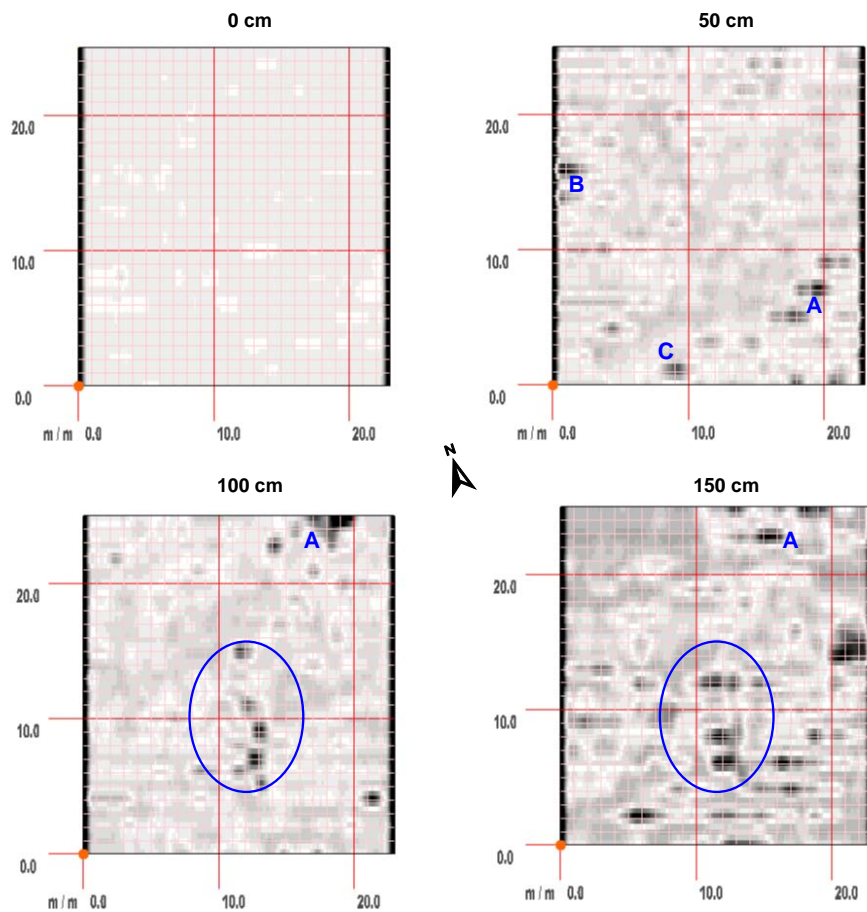


Figure 13. Time-sliced images from Grid 1 at the Harriet Beecher House

In Figure 13, the shallowest (0 cm) slice reveals low amplitudes reflections that signify similar materials. In the 50 cm slice, a series of high amplitude reflections extend across the southeast portion of the grid and between “A” and “C”. These reflections may be from separate features and/or represent a linear feature that has been poorly captured with GPR. If a linear feature exists between these points, the large distance between the successive traverse lines (1-m) and mistiming of reference marks on the radar record could account for the segmented appearance and poor alignment of these reflections. Also in the 50 cm slice are several high

amplitude reflections near “B.” The areas specified may be of interest and should be mentioned to historians and archaeologists concerned with this site.

In the 100 and 150 cm slices, high amplitude signals persist in both slices in the northeast corner near “A” and the area outlined by the blue oval. Trees and shrubs adjoin the northern side of the grid area near “A.” Although the exact location of this vegetation was not properly noted, the source of the high amplitude reflections in this portion of the grid may be tree roots. The area defined by the oval is located in the center of the lawn. This area is a good candidate for remnants from the former greenhouse, which is believed to have occupied this general area. These areas may be worthy of future investigations by archaeologists.

### Grid 2

Figure 14 is a three-dimensional block image of the shallow subsurface beneath Grid 2 at the Harriet Beecher House. A large inset has been removed from this block to enable an improved viewing of the underlying strata. Compare with Grid 1, Grid 2 covered an area that is underlain by several well expressed strata. The high amplitude, planar reflectors in the lower part of the radar record most likely represent strata of contrasting lacustrine clays and silts from Glacial Lake Hitchcock.

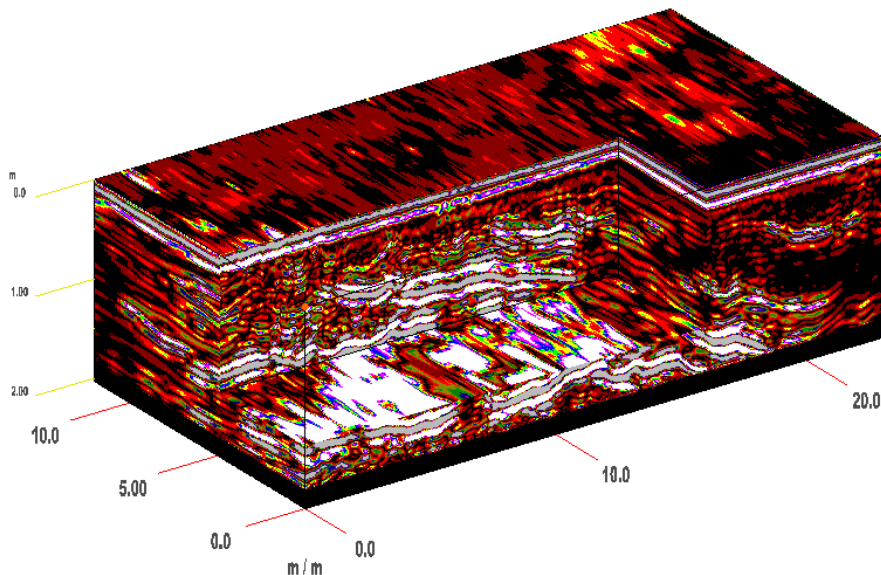


*Figure 14. Three-dimensional block diagram showing the strata that underlies Grid 2 at the Harriet Beecher House*

Figure 15 contains four time-slice images of Grid 2. In Figure 15, all measurements are expressed in meters. The origin is located in the lower left-hand corner (southwest corner of grid area) of each slice. The four horizontal “time-slices” represent depths of about 0, 50, 100, and 150 cm. These depths were based on an averaged signal propagation velocity of 0.10 m/ns through the soil. The width of the time-slice is about 12 cm. The dark vertical lines along the west (left) and east (right) boundaries of each time-slice image are artifacts of the processing techniques used.

In Figure 15, the shallowest (0 cm) slice reveals low to moderate amplitude reflections across all but the southwest portion of the grid area, where the amplitudes are moderately high. The moderately high amplitudes in the southwest portion may be due to dissimilar fill materials which appear to be aligned in a generalized north to south pattern. In the 50 cm slice, a chaotic pattern of moderately high amplitude reflections extend across western portion of the grid. Chaotic patterns also characterize the 100 and 150 cm slices, where high amplitudes

reflections become more extensive. These chaotic patterns are associated with the subsurface strata evident in Figure 14. In the 100 and 150 cm slices, the large area of nondescript, moderate amplitude reflections (dark gray) that dominates the eastern portion of the grid is associated with recent fill materials.

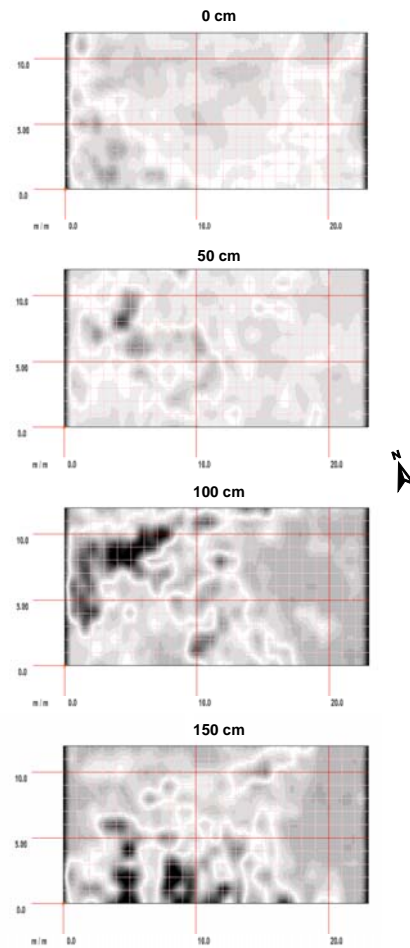


*Figure 15. Time-sliced images from Grid 2 at the Harriet Beecher House*

## References

- Bevan, Bruce W. 1991. The search for graves. *Geophysics* 56(9):1310-1319.
- Bevan, B. and J. Kenyon. 1975. Ground-probing radar for historical archaeology. *MASCA (Museum Applied Science Center for Archaeology) University of Pennsylvania, Philadelphia. Newsletter* 11(2): 2-7.
- Bruzewicz, A. J., C. R. Smith, D. E. Berwick, and J. E. Underwood. 1986. The use of ground-penetrating radar in cultural resource management. *Technical Papers 1986 ACSM-ASPRS Annual Convention Vol. 5: 233-242.*
- Brune, D. E. and J. A. Doolittle. 1990. Locating lagoon seepage with radar and electromagnetic survey. *Environ. Geol. Water Sci.* 16:195-207.
- Conyers, L. B., and D. Goodman. 1997. *Ground-penetrating Radar; an introduction for archaeologists.* AltaMira Press, Walnut Creek, CA.

- Dalan, R. 1990. Defining archaeological features with electromagnetic surveys at the Cahokia Mounds State Historic Site. *Geophysics* 56(8): 1280-1287.
- Daniels, D. J. 1996. *Surface-Penetrating Radar*. The Institute of Electrical Engineers, London, United Kingdom.
- Dolphin, L. and T. J. Yetter. 1985. Geophysical survey at Third Mission Site, Santa Clara University. SRI Project 8745. SRI International, Menlo Park, California.
- Doolittle, J. A. 1987. Using ground-penetrating radar to increase the quality and efficiency of soil surveys. pp. 11-32. In: Reybold, W. U. and G. W. Peterson (eds.) *Soil Survey Techniques*, Soil Science Society of America. Special Publication No. 20.
- Doolittle, J. A. 1988. Ground-penetrating radar (GPR) survey at Tell Halif, Israel. pp. 180-213. In: *Technical Proceedings of the Second International Symposium on Geotechnical Applications of Ground-Penetrating Radar*. Gainesville, Florida. March 6-10 1988.
- Drommerhausen, D. J., D. E. Radcliffe, D. E. Brune, and H. D. Gunter. 1995. Electromagnetic conductivity survey of dairies for groundwater nitrate. *J. Environmental Quality*, 24: 1083-1091.
- Eigenberg, R. A., R. L. Korthals, and J. A. Nienaber. 1998. Geophysical electromagnetic survey methods applied to agricultural waste sites. *J. Environmental Quality*, 27:215-219.
- Frohlich, B. and W. J. Lancaster, 1986. Electromagnetic surveying in current Middle Eastern archaeology: Applications and evaluation. *Geophysics* 51: 1414-1425.
- Goodman, D., S. Piro, Y. Nishimura, H. Patterson. 2004. Discovery of a 1<sup>st</sup> century AD Roman amphitheater and other structures at the Forum Novum by GPR. *Journal of Environmental & Engineering Geophysics*, 9(1): 35-41.
- Gracia, V. P., J. A. Canas, L. G. Pujades, J. Clapes, O. Caselles, F. Garcia, and R. Osorio. 2000. GPR survey to confirm the location of ancient structures under Valencian Cathedral (Spain). *Journal of Applied Geophysics* 43: 167-174.
- Greenhouse, J. P., and D. D. Slaine. 1983. The use of reconnaissance electromagnetic methods to map contaminant migration. *Ground Water Monitoring Review* 3(2):47-59.
- Ilgen, L. W., A. W. Benton, K. C. Stevens, Jr., A. E. Shearin, and D.E. Hill 1969. *Soil Survey of Tolland County, Connecticut*. USDA-SCS in cooperation with the Connecticut Agricultural Experiment Station and the Storrs Agricultural Experiment Station. US Government Printing Office, Washington, DC.
- Kachanoski, R. G., E. G. Gregorich, and I. J. Van Wesenbeeck. 1988. Estimating spatial variations of soil water content using noncontacting electromagnetic inductive methods. *Can. J. Soil Sci.* 68:715-722.
- Killam, E. W. 1990. *The detection of human remains*. Charles C. Thomas Publisher, Springfield, Illinois.
- King, J. A., B. W. Bevan, and R. J. Hurry. 1993. The reliability of geophysical surveys at historic-period cemeteries: An example from plains Cemetery, Mechanicsville, Maryland. 1993. *Historical Archaeology* 27(3): 4-16.
- McNeill, J. D. 1980. *Electrical Conductivity of soils and rocks*. Technical Note TN-5. Geonics Ltd., Mississauga, Ontario.
- McNeill, J. D. 1996. Why doesn't Geonics Limited build a multifrequency EM31 or EM38 meter? Technical

Note TN-30. Geonics Limited, Mississauga, Ontario.

Morey, R. M. 1974. Continuous subsurface profiling by impulse radar. 212-232 pp. IN: Proceedings, ASCE Engineering Foundation Conference on Subsurface Exploration for Underground Excavations and Heavy Construction, held at Henniker, New Hampshire. Aug. 11-16, 1974.

Pipan, M., L. Baradello, E. Forte, A. Prizzon, and I. Finetti. 1999. 2-D and 3-D processing and interpretation of multi-fold ground penetrating radar data: a case history from an archaeological site. *Journal of Applied Geophysics* 41: 271-292.

Radcliffe, D. E., D. E. Brune, D. J. Drohmerhausen, and H. D. Gunther. 1994. Dairy loafing areas as sources of nitrate in wells. p. 307-313. IN: Environmentally Sound Agriculture; Proceedings of the Second Conference. 20-24 July 1994. American Society of Agricultural Engineers. St. Joseph, MI.

Ranjan, R. S., and T. Karthigesu. 1995. Evaluation of an electromagnetic method for detecting lateral seepage around manure storage lagoons. ASAE Paper 952440. ASAE, St. Joseph, MI.

Reynolds, C. 1979. Soil Survey of New Haven County, Connecticut. USDA – Soil Conservation Service in cooperation with the Connecticut Agricultural Experiment Station and Storrs Agricultural Experiment Station. US Government Printing Office, Washington, DC.

Rhoades, J. D., P. A. Raats, and R. J. Prather. 1976. Effects of liquid-phase electrical conductivity, water content, and surface conductivity on bulk soil electrical conductivity. *Soil Sci. Soc. Am. J.* 40:651-655.

Shearin, A. E., and D. E. Hill. 1962. Soil Survey of Hartford County, Connecticut. USDA – Soil Conservation Service in cooperation with the Connecticut Agricultural Experiment Station and Storrs Agricultural Experiment Station. US Government Printing Office, Washington, DC.

Siegrist, R. L. and D. L. Hargett. 1989. Application of surface geophysics for location of buried hazardous waste. *Water Management and Research* 7:325-335.

Stierman, D. L. and L. C. Ruedisili. 1988. Integrating geophysical and hydrogeological data: An efficient approach to remedial investigations of contaminated ground water. p. 43-57. IN: Collins, A. G. and A. J. Johnson (eds.) *Ground water contamination field methods*. ASTM STP 963. American Society for Testing Materials, Philadelphia.

Vaughan, C. J. 1986. Ground-penetrating radar surveys in archaeological investigations. *Geophysics* 51(3): 595-604.

Vickers, R., L. Dolphin, and D. Johnson. 1976. Archaeological investigations at Chaco Canyon using subsurface radar. 81-101 pp. IN: *Remote Sensing Experiments in Cultural Resource Studies*, assembled by Thomas R. Lyons, Chaco Center, USDI-NPS and University of New Mexico.

Whiting, B. M. D., McFarland, D. P., S. Hackenberger. 2000. Preliminary results of three-dimensional GPR-based study of a prehistoric site in Barbados, West Indies. 260-267 pp. IN: (Noon, D. ed.) *Proceedings Eight International Conference on Ground-Penetrating Radar*. May 23 to 26, 2000, Goldcoast, Queensland, Australia. The University of Queensland.

Won, I. J. 1996. A wideband electromagnetic exploration method - Some theoretical and experimental results. *Geophysics* 45:928-940